

# Assessment of Preliminary Prediction Techniques for Wing Leading-Edge Vortex Flows at Supersonic Speeds

Richard M. Wood\* and David S. Miller\*  
NASA Langley Research Center, Hampton, Virginia

A theoretical investigation of the aerodynamics of sharp leading-edge delta wings at supersonic speeds has been conducted. The primary objective of this study was to determine the applicability of existing theoretical methods to predict wing leading-edge separated-flow characteristics at conditions conducive to high-lift supersonic flight. Predicted results from two modified linear-theory methods (LTSTAR and VORCAM) are compared with experimental data. Comparison of the two methods for uncambered wings revealed that the LTSTAR code is in much better agreement with experimentally measured vortex strength, vortex position, and total lifting characteristics than the VORCAM code. Selected analysis was also performed with an Euler code, SWINT. The results of this study indicated that the SWINT code was not well suited to the analysis of wings with separated flow at high lift and low supersonic speeds.

## Nomenclature

$\Delta C_A$	= incremental change in axial force coefficient, = $C_A - C_A _{\alpha=0 \text{ deg}}$
$\Delta C_D$	= incremental change in drag coefficient from the minimum drag of a flat wing
$C_L$	= lift coefficient
$\Delta C_L$	= nonlinear incremental change in lift coefficient with respect to linear lift coefficient, = $C_L _{\alpha=20 \text{ deg}}$ - $(20)C_{L\alpha}$
$C_{L\alpha}$	= lift-curve slope
$C_N$	= normal-force coefficient
$C_N^l, C_N^u$	= wing lower- and upper-surface normal-force coefficient
$C_{N,v}$	= vortex strength
$C_p$	= pressure coefficient
$c_{LE}$	= local chord of deflected portion of wing leading edge
$M$	= Mach number
$M_N$	= component of Mach number normal to wing leading edge, = $M \cos \Lambda_{LE} (1 + \sin^2 \alpha \tan^2 \Lambda_{LE})^{1/2}$
$x, y, z$	= Cartesian coordinates
$\alpha$	= angle of attack
$\alpha_N$	= angle of attack normal to wing leading edge, = $\tan^{-1}(\tan \alpha / \cos \Lambda_{LE})$
$\beta$	= $\sqrt{M^2 - 1}$
$\delta_{LE}$	= flap deflection angle, positive leading edge down
$\eta$	= fraction of local wing semispan
$\eta_v$	= semispan location of vortex action point
$\Lambda_{LE}$	= wing leading-edge sweep angle

## Introduction

IN the past, aerodynamicists have employed linear-theory-based methods for the design of twisted and cambered wings for efficient low-lift supersonic flight.<sup>1,2</sup> At these low-lift conditions, the inviscid linearized potential equation has proved to be adequate for the analysis and design of complex geometries. However, as the design lift coefficient is in-

creased, the ability of the linear-theory-based methods to model the complex flowfield of a configuration degrades. At high-lift conditions, the flow becomes extremely nonlinear requiring the use of higher-order prediction techniques which take into account the various nonlinear flow phenomenon in determining the configuration aerodynamics.

The first research efforts which investigated the high-lift flow regime were guided by the theoretical development of a fully three-dimensional inviscid, attached-flow computational approach which employed the full-potential equation. This wing-design study made use of supercritical cross-flow with a shockless recompression to maintain attached flow over the wing upper surface to minimize the drag at a design lift coefficient of 0.4. The attached-flow high-lift wing-design concept has been extensively documented,<sup>3</sup> however, the performance improvements attained in the study may be susceptible to inherent minimum drag penalties due to camber and thickness and may be susceptible to boundary-layer separation at off-design conditions. An alternate high-lift wing-design concept being proposed would use a controlled leading-edge vortex flow positioned on the proper wing camber surface to produce both lift and aerodynamic thrust. The design of such a wing surface is a severe challenge to the aerodynamic community due to the computational complexity involved in modeling the wing flowfield (Fig. 1). Unlike the attached-flow solution in which the viscous effects could be accounted for separately in the wing-design cycle, the vortex flowfield does contain an interaction between the viscous boundary layer and the inviscid freestream flow.

Although over the past few years various nonlinear, separated-flow, computer codes (Euler and Navier-Stokes) have been developed to treat this problem, the majority of these computer codes are not well suited to preliminary design studies. As a result, this paper will review the capabilities of a single Euler and two modified linear-theory separated-flow prediction methods. The ability of each code to model the characteristics of the vortex as well as predict the aerodynamics of both flat and cambered delta wings will be investigated.

## Discussion

### Review of the Fundamental Aerodynamic Characteristics of Delta Wings

To put the theoretical analysis of this paper into perspective, the fundamental aerodynamic characteristics of delta wings with leading-edge vortex flow will be reviewed. The

Presented, in part, as Paper 84-2208 at the AIAA 2nd Applied Aerodynamics Conf., Seattle, Wash., Aug. 21-23, 1984; received Aug. 31, 1984; revision received March 15, 1985. This paper is declared a work of the U.S. Government and therefore is in the public domain.

\*Aero-Space Technologist, Fundamental Aerodynamics Branch, High-Speed Aerodynamics Division. Member AIAA.

supersonic aerodynamics of delta wings with subsonic, sharp leading edges have been documented extensively. In 1954 and 1963, Brown and Michael<sup>4</sup> and Squire et al.<sup>5</sup> respectively, identified that nonlinear lift does occur at supersonic speeds, but only for combinations of low Mach number and high wing leading-edge sweep conditions. In 1955, Love<sup>6</sup> showed that the variation in experimental lift-curve slope (shaded band in Fig. 2) with the parameter  $\beta \cot \Lambda_{LE}$  is different from that predicted by linear theory for values of  $\beta \cot \Lambda_{LE} > 0.50$ . The data of Fig. 2 show that for values of  $\beta \cot \Lambda_{LE}$  greater than 0.50, the experimental lift-curve slope remains constant. These results suggest that wing designs employing the separated-flow concept should be performed for  $\beta \cot \Lambda_{LE}$  between 0.50 and 0.70. Recent results by Miller and Wood<sup>7</sup> expanded on the work of Stanbrook and Squire<sup>8</sup> by identifying and categorizing six distinct attached- and separated-flow conditions that occur on the leeside of delta wings (Fig. 3). Based upon these flow categories, Miller and Wood suggested that future separated-flow wing design should be performed for  $M_N < 0.9$  and  $\alpha_N$  from 10 to 40 deg. Within these bounds, the data of Ref. 7 indicated that a classical wing leading-edge vortex would form and produce a significant amount of vortex-induced suction force that could be used for drag minimization. In 1984, Wood and Miller<sup>9</sup> showed that there is a highly nonlinear shifting of lift from the upper surface (vortex lift) to the lower surface (compression lift) with increasing Mach number and angle of attack. Figures 4 and 5 illustrate the upper- and lower-surface normal-force behavior, respectively, for flat delta wings. The results of Figs. 4 and 5 can be combined to show how the upper- and lower-surface normal forces contribute to the total wing-lifting characteristics. Depicted in Fig. 6 are two graphical representations of the lifting characteristics of delta wings at supersonic speeds. The sketch on the left reflects the "subsonic analogy" which assumes that the vortex produces all of the nonlinear lift; however, the nonlinear lift increment between linear theory and experiment is actually due to a combination of both upper- and lower-surface nonlinear characteristics (right side of Fig. 6). These results in Figs. 4-6 provide an excellent set of correlated ex-

perimental data that will be used later in this paper to evaluate the capabilities of the theoretical methods.

### Nonlinear Methods

In 1983, Hitzel and Schmidt<sup>10</sup> indicated that the Euler codes could become the next generation of codes for predicting separated flows. The applicability of the Euler equations to the solution of the flowfields about sharp leading-edge wings at angle of attack is still questioned by the aerodynamic community.<sup>11</sup> Even though the highly complex viscous-inviscid interaction is not represented by the Euler equations, the Euler equations may be able to model the characteristics of the

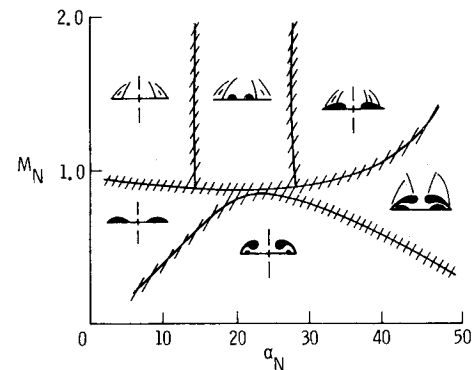


Fig. 3 Flat delta wing leeside flow characteristics.

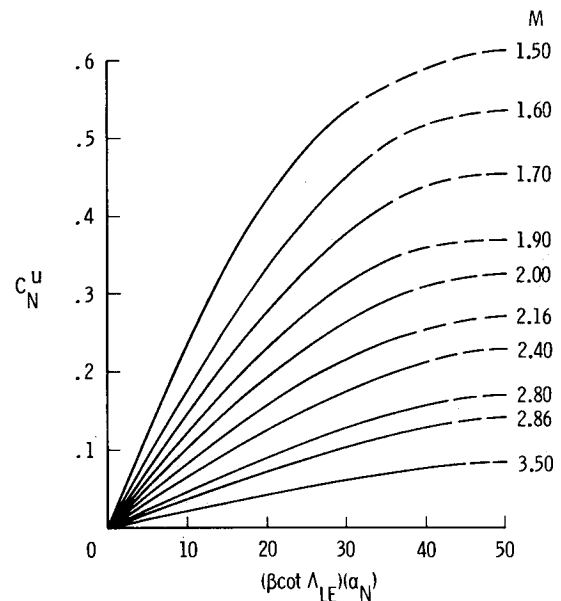


Fig. 4 Flat delta wing upper-surface normal-force characteristics.

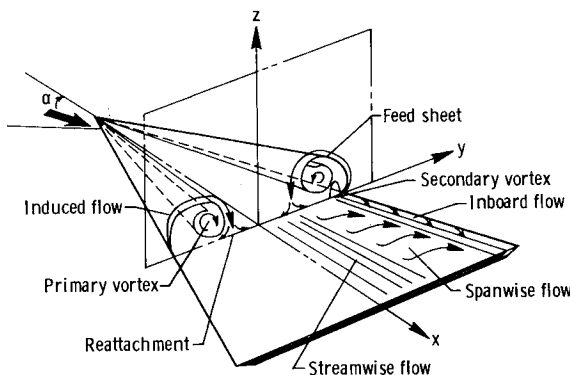


Fig. 1 Wing leading-edge vortex flow characteristics.

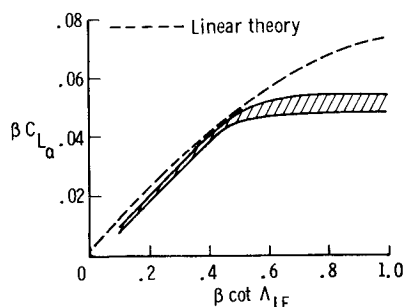


Fig. 2 Flat delta wing lifting characteristics.

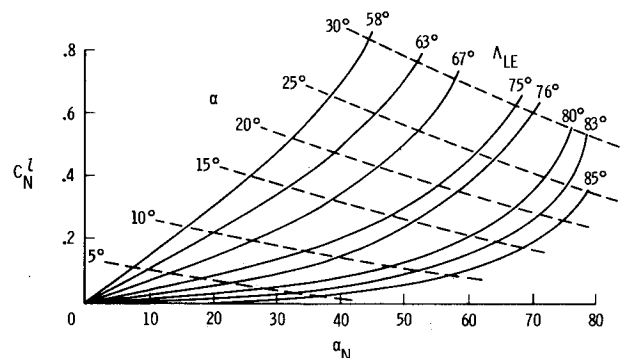


Fig. 5 Flat delta wing lower-surface normal-force characteristics.

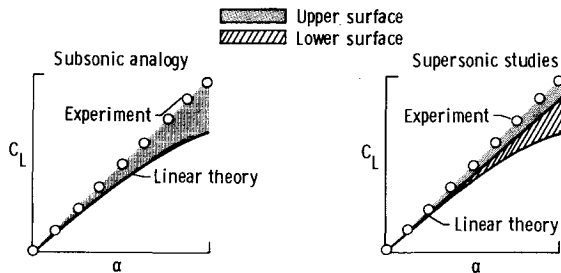


Fig. 6 Vortex-induced lifting characteristics of flat delta wings at supersonic speeds.

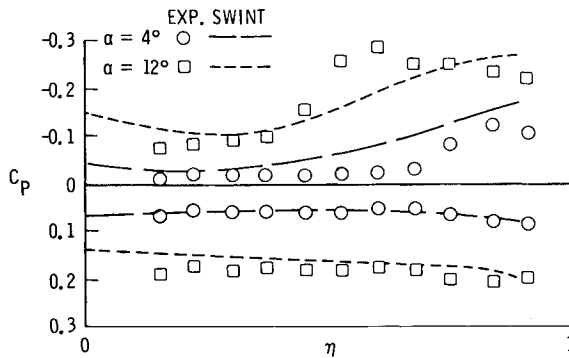


Fig. 7 Experimental and SWINT-predicted spanwise pressure distributions for a 75 deg delta wing at  $M=1.90$ .

flowfield to a satisfactory level to allow design studies to be conducted. To determine the applicability of nonlinear prediction techniques for the analysis of wings at high lift conditions and having separated-flow, several user-friendly, well-documented Euler and Navier-Stokes codes, with high levels of computational flexibility, were reviewed. Based upon this review, an Euler code "SWINT,"<sup>12</sup> was selected for evaluation. The SWINT code was developed for the analysis of tactical missile configurations and is an explicit finite difference method that uses a thin-wing approximation. In the evaluation of the SWINT code, a variety of flat delta wing geometries were analyzed over a broad range of Mach numbers and angles of attack. Predicted pressure, flowfield, and force results, along with experimental data, are shown in Figs. 7-10.

Figure 7 shows two angles of attack for comparison between SWINT predicted and experimentally measured spanwise pressure distributions for a 75 deg delta wing at  $M=1.90$ . In the experimental upper-surface pressure distributions, the position of the vortex is clearly indicated by the localized increase in suction pressure. The experimental data show that at 4-deg angle of attack the vortex is located at 80% of the semispan and at 12-deg angle of attack the vortex has moved inboard to 60% of the semispan. The SWINT-predicted results depict a much different character of upper-surface flowfield. The vortex-induced suction pressures observed in the experimental data are not evident in the theory. For both 4- and 12-deg angles of attack, the SWINT results show a gradual increase in upper-surface suction pressures as the wing leading edge is approached; this character is representative of an attached-flow condition. To determine the nature of the wing flowfield, the predicted flowfield for 12-deg angle of attack is presented in Fig. 8. Cross-flow velocity vectors are presented in Fig. 8 for the 75 deg delta wing at 12-deg angle of attack. The plot clearly shows rotational flow above the wing surface. The center of the vortical structure observed in the cross-plane plot correlated well with the vortex location extracted from the data.

The ability of the SWINT code to predict the isolated vortex characteristics will be established next. The experimental and

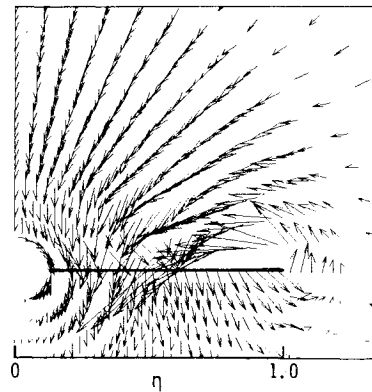


Fig. 8 SWINT predicted cross-flow velocity vectors for a 75 deg delta wing at  $\alpha = 12$  deg,  $M = 1.90$ , and  $x/l = 0.8$ .

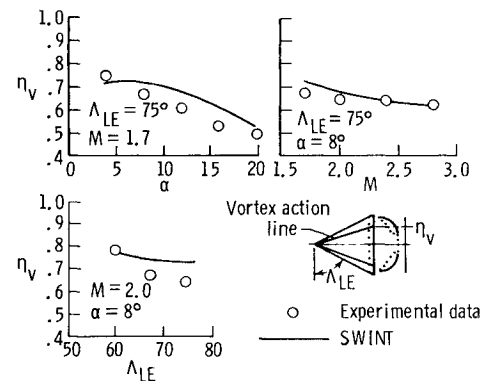


Fig. 9 SWINT-predicted and experimentally measured effect of Mach number, angle of attack, and leading-edge sweep on the vortex position for flat delta wings.

theoretical vortex strength ( $C_{N,v}$ ) and vortex location ( $\eta_v$ ) are extracted from spanwise pressure distributions by an integration of the difference between the upper-surface attached-flow surface pressure distribution (predicted by linear theory) and the experimentally measured separated-flow pressure distribution.

The effects of angle of attack, Mach number, and leading-edge sweep on the vortex position are shown in Fig. 9. The trend of the experimental data is an inboard movement of the vortex with increasing angle of attack, Mach number, and wing leading-edge sweep. As indicated by both experimental and SWINT results, the most pronounced effect is seen for a change in angle of attack. The vortex moves from the 80% semispan position to the 50% semispan position as angle of attack changes from 4 to 20 deg. All observed changes in vortex location are predicted by the SWINT code.

The effect of increasing Mach number and angle of attack on vortex strength is presented in Fig. 10. The experimental data show that vortex strength decreases with an increase in Mach number and increases with increasing angle of attack. Typically, the vortex strength will decrease continually with an increase in Mach number until  $M_N$  becomes greater than 1.0 or until the wing upper-surface suction pressures reach the vacuum limit. Similarly, the vortex strength will increase continually with an increase in angle of attack until the upper-surface suction pressures near the vacuum limit. The SWINT code failed to predict any of these trends. In general, the analysis showed an inability of the SWINT code to predict the separated-flow characteristics and vortex-induced aerodynamics within the range of Mach number and angle of attack previously defined as the feasible high-lift, separated-flow, design space. However, excellent agreement between theory and experiment was obtained at higher Mach numbers ( $M > 2.0$ ).

Presented in Fig. 11 is a sketch showing the region of acceptable solutions obtained from the SWINT code for sharp leading-edge delta wings (shaded region). The results of this study indicate that this particular Euler code,<sup>16</sup> although extremely user friendly, is not well suited to the analysis of wings with separated flow at low to moderate supersonic speeds ( $M_N < 0.9$ ). These results are not intended to be generally applicable to all Euler codes, but are rather specific and apply to the SWINT code only. A further review of the literature uncovered a wide range of opinions on the applicability of Euler codes to the analysis of wing leading-edge separated flow.<sup>13,14</sup>

In summary, before the true potential of a high-lift, separated-flow, supersonic wing design can be assessed, the development of nonlinear analysis/design methods is required. These methods would fill a significant void in the existing aerodynamic analysis capabilities.

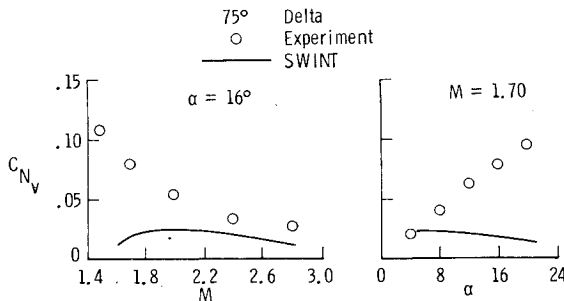


Fig. 10 SWINT-predicted and experimentally measured effect of Mach number and angle of attack on the vortex strength for flat delta wings.

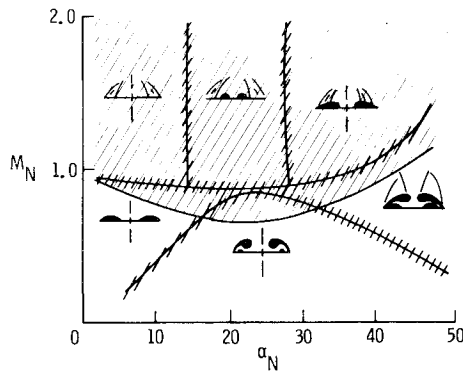


Fig. 11 Evaluation of SWINT code.

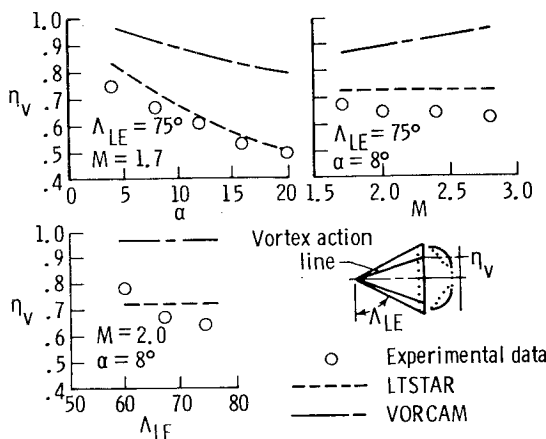


Fig. 12 Modified linear-theory-predicted and experimentally measured effect of Mach number, angle of attack, and leading-edge sweep on the vortex position for flat delta wings.

### Modified Linear Theory Methods

The majority of the original separated-flow prediction methods were based upon linear theory<sup>4</sup> and failed to account for the effect of compressibility at supersonic speeds. In 1966, Polhamus derived the leading-edge suction analogy for subsonic flows and, in 1971, extended his analogy to supersonic speeds.<sup>15</sup> This provided the supersonic aerodynamicists with a separated-flow prediction method for uncambered wings having straight leading edges. In 1980 and 1981, Carlson and Mack<sup>16</sup> and Lan and Chang,<sup>17</sup> respectively, refined and extended the application of the full-suction analogy to cambered wings having arbitrary planforms.

The Carlson code, LTSTAR,<sup>16</sup> is a linearized-theory method modified to account for both nonlinear attached-flow effects (lower surface) and nonlinear separated-flow effects (upper surface). The leading-edge separated flow is represented by a technique which uses the Polhamus suction analogy to determine the leading-edge separated-flow force and then modifies the upper-surface attached-flow pressures to distribute this additional force over the wing upper surface. The separated-flow force is distributed about a "vortex action point" located downstream of the wing leading edge. In this code, the vortex action point is determined from an empirical relationship that is a function of angle of attack only. The code also corrects the upper-surface lift force by limiting the distributed pressure values to the vacuum limit. The Lan code, VORCAM,<sup>17</sup> is also a linearized-theory method modified to account for the nonlinear separated-flow effects (upper surface). This method uses the Polhamus suction analogy in combination with a semiempirical relationship to determine the suction force. The suction force is then positioned aft of the wing leading edge at a distance determined through consideration of the momentum principle. This second method does not attempt to distribute the suction force or limit the upper-surface lift force in any manner.

The ability of the two later modified linear theory computer codes to predict the isolated vortex characteristics as well as the longitudinal aerodynamics of delta wings will now be determined. As was done for the SWINT code, the evaluation of these two codes is based upon a comparison of pressure and force data and the ability of each code to model the location and strength of a wing leading-edge vortex.

The evaluation of both aerodynamic analysis codes was limited to delta wings with leading-edge sweep angles of 60 to 75 deg, Mach numbers of 1.4 to 2.8, and angles of attack of 0 to 20 deg. In each case, the codes were applied in a conventional and consistent manner to evaluate their treatment of leading-edge vortex flows. Shown in Figs. 12-14 are representative results of this analysis.

The effects of angle of attack, Mach number, and leading-edge sweep on the vortex position for flat delta wings are shown in Fig. 12. As indicated by both experimental and theoretical results, the most pronounced effect is seen for a change in angle of attack. These changes in vortex location

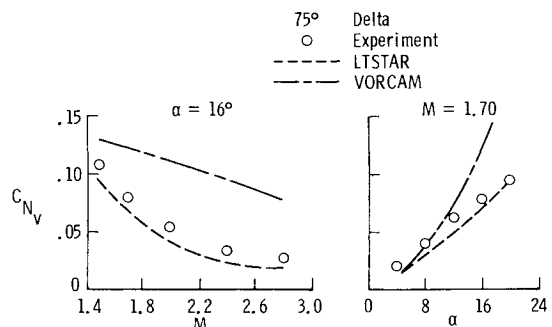


Fig. 13 Modified linear-theory-predicted and experimentally measured effect of Mach number and angle of attack on the vortex strength for flat delta wings.

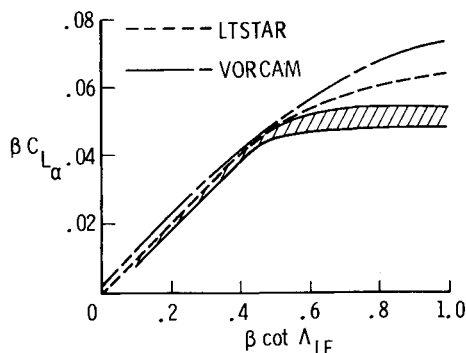


Fig. 14 Predicted lifting characteristics for flat delta wings.

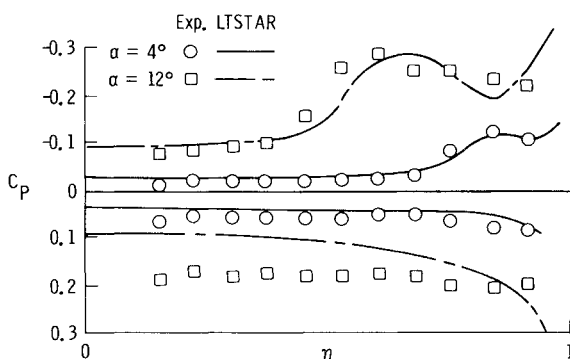


Fig. 15 Experimental and LTSTAR-predicted spanwise pressure distributions for a 75-deg wing at  $\alpha = 12^\circ$ ,  $M = 1.90$ , and  $x/\ell = 0.8$ .

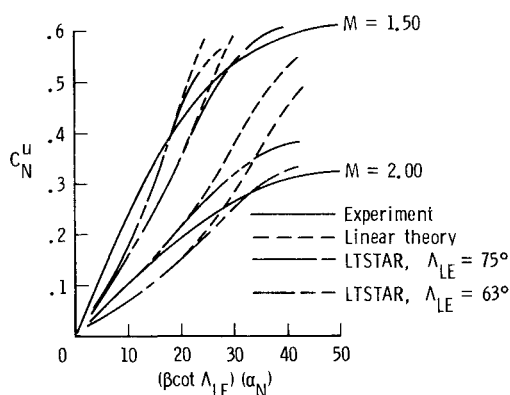


Fig. 16 Measured and predicted flat delta wing upper-surface normal-force characteristics.

with angle of attack are predicted by the LTSTAR code, and not by the VORCAM code. A comparison of the computed results with experimental data for changes in Mach number and leading-edge sweep shows similar results; the LTSTAR code predicts both the position and trend of the vortex. The VORCAM code consistently locates the vortex too near the wing leading edge, and the method actually predicts an outboard progression of the vortex for an increase in Mach number. In general, the experimental vortex location is usually inboard of the predicted location for both methods.

Presented in Fig. 13 is the effect of increasing Mach number and angle of attack on vortex strength. The effect of changes in wing leading-edge sweep on vortex strength was small and is not discussed herein. Theoretical predictions by the LTSTAR code are in much closer agreement with the experimental data than the VORCAM predictions. The good correlation between the LTSTAR code and the experimental data can be attributed

to the treatment of the vortex strength within the code (i.e., distribution and vacuum limit). The VORCAM code consistently overpredicts the vortex strength and does not predict the correct variation of vortex strength with either changes in Mach number or changes in angle of attack. The most significant discrepancy exhibited by the VORCAM code is the quadratically increasing vortex increment with angle of attack. Although this quadratically increasing vortex increment would be expected by a direct application of the Polhamus suction analogy, there is no evidence of this vortex behavior in the experimental data.

The predicted lifting characteristics for flat delta wings with leading-edge separation are summarized in Fig. 14. The data show that for  $\beta \cot \Lambda_{LE}$  values less than 0.50, both methods agree with the experimental data. For  $\beta \cot \Lambda_{LE}$  values greater than 0.50, both methods overpredict the lift-curve slope parameter and fail to predict its leveling-off character.

The results of Figs. 12-14 indicate that the LTSTAR code is in much better agreement with experimental data than the VORCAM code in predicting the isolated vortex characteristics and the lifting characteristics of delta wings. In addition, the LTSTAR code treats the vortex force increment in a realistic fashion by distributing vortex-induced pressures and it also modifies the lower-surface pressures to account for nonlinear compression effects. To evaluate both of these nonlinear corrections, LTSTAR predicted pressure distributions and wing upper- and lower-surface normal-face characteristics are compared to experimental data in Figs. 15-17.

The predicted upper-surface pressure distributions of Fig. 15 are in excellent agreement with the experimental data; however, the lower-surface pressures predicted by the LTSTAR code are lower than the experimental data. This lower-surface behavior is typical of a linear-theory-based solution. An important point to notice in these results is that the leading-edge singularity in the pressure distribution remains large and unaffected by the superposition of the linear-theory solution and the nonlinear corrections. At high angles of attack, these large leading-edge pressures significantly influence the individual upper- and lower-surface normal forces as seen in Figs. 16 and 17.

Presented in Fig. 16 is a comparison of the predicted and measured upper-surface normal-force characteristics for uncambered delta wings. Experimental and theoretical results are shown for Mach numbers of 1.50 and 2.00. Each experimental curve is comprised of a range of wing leading-edge sweeps between 58 and 85 deg. When correlated in the same way, the predicted data failed to collapse into a single curve which was independent of leading-edge sweep. As a result, LTSTAR results for only two leading-edge sweeps of 63 and 75 deg are presented. Linear-theory predictions taken from the LTSTAR code are also presented for comparison. The LTSTAR predictions show a large effect of sweep, angle of attack, and Mach number on the upper-surface normal force. At low angles of attack, the predicted normal force is less than that observed experimentally, however, as the correlation parameter is increased the theoretical and experimental curves cross. The figure also shows that increasing wing sweep delays the crossover to a higher value of the correlation parameter. The LTSTAR results show considerable improvement over the linear-theory results, especially at high angles of attack and high Mach numbers.

The predicted and measured wing lower-surface normal-force characteristics are presented in Fig. 17. The data shows that the lower-surface corrections in the LTSTAR code improve the linear-theory predictions (dashed line) at high angles of attack and for large wing leading-edge sweeps.

The results of Figs. 16 and 17 show that the capability of the LTSTAR code to predict the individual upper- and lower-surface normal-force coefficient is inconsistent with variations in angle of attack, Mach number, and wing leading-edge sweep. The code failed to predict the effect of wing sweep on

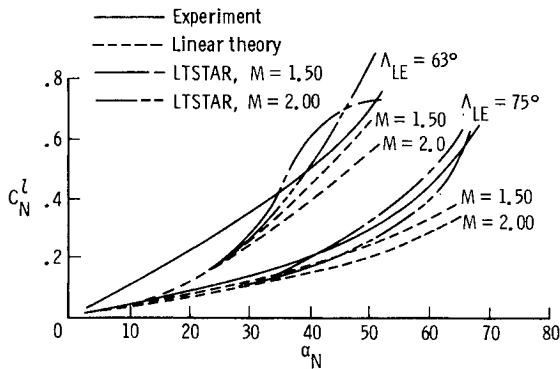


Fig. 17 Measured and predicted flat delta wing lower-surface normal-force characteristics.

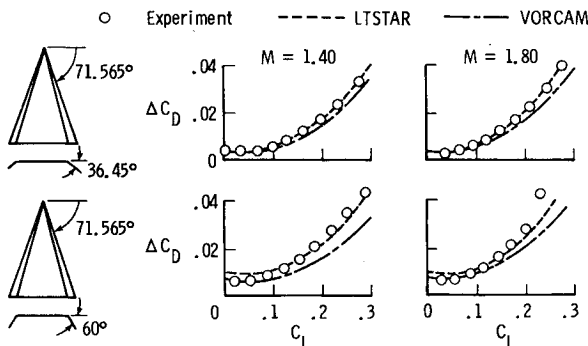


Fig. 18 Predicted drag-due-to-lift characteristics for cambered delta wings.

the upper-surface normal-force characteristics. In addition to the data of Figs. 16 and 17, the data of Figs. 13 and 14 also show that the effect of wing sweep was not accounted for properly in the prediction of either vortex position or strength. These effects must be reproduced properly to attain a reliable vortex-flow prediction technique.

To illustrate the ability of the two modified linear-theory codes to predict supersonic vortex-flap performance, experimental and theoretical drag-due-to-lift polars are shown in Fig. 18 for a delta wing ( $\Lambda_{LE} = 71.565^\circ$ ) with a conical leading-edge flap comprising the outboard 15% of the local semispan. At Mach numbers of 1.40 and 1.80, results are presented for flap deflection angles of 36.45 and 60 deg, as shown in the sketches. The LTSTAR code predictions are in excellent agreement with experimental data, and the VORCAM code underpredicts the drag due to lift for lift-coefficient values above 0.10. These results can be explained by information shown in Figs. 12 and 13. The flat-wing analysis revealed that the VORCAM code consistently positioned the leading-edge vortex too near the wing leading edge and overpredicted the vortex strength. The combination of these effects, although not critical in the analysis of flat wings, allows the overpredicted suction force to remain on the forward-facing deflected leading edge to a higher angle of attack. In summary, the VORCAM code will consistently produce optimistic drag values for wings with deflected leading edges because it does not distribute or limit the suction force and because it locates the vortex too near the wing leading edge.

### Concluding Remarks

A theoretical investigation of the aerodynamic of sharp leading-edge delta wings at supersonic speeds has been conducted. The supporting experimental data for this investigation were taken from published force, pressure, and flow-visualization data in which the Mach number normal to the wing leading edge is always less than 1.0. The primary objective of this study was to determine the applicability of existing theoretical methods to predict wing leading-edge separated-

flow characteristics at conditions conducive to high-lift supersonic flight.

Experimental data were compared with predicted results from two modified linear-theory methods. Comparison of the two methods for uncambered delta wings revealed that the LTSTAR code is in much better agreement with experimentally measured vortex strength, vortex position, and total lifting characteristics than the VORCAM code. The VORCAM code consistently overpredicted the vortex strength and positioned the vortex too near the wing leading edge. The impact of this incorrect treatment of the vortex by the VORCAM code was most evident in the analysis of wings with deflected leading-edge flaps. The VORCAM code underpredicted the drag due to lift consistently, whereas the LTSTAR code results were in better agreement with the experimental data. Selected analysis was also performed with the SWINT Euler code. These results indicated that the SWINT code was not well suited to the analysis of wings with separated flow at high lift and low supersonic speeds.

### Acknowledgment

O. J. Rose of Kentron International has made significant contributions to the theoretical analysis presented in this report. His work is gratefully acknowledged.

### References

- Carlson, H. W., "Aerodynamic Characteristics at Mach Numbers 2.05 of a Series of Highly-Swept Arrow Wings Employing Various Degrees of Twist and Camber," NASA TM X-332, 1960.
- Miller, D. S. and Schemensky, R. T., "Design Study Results of a Supersonic Cruise Fighter Wing," AIAA Paper 79-0062, Jan. 1979.
- Miller, D. S., Pittman, J. L., and Wood, R. M., "An Overview of Non-linear Supersonic Wing-Design Studies," AIAA Paper 83-0182, Jan. 1983.
- Brown, C. E. and Michael, W. H., "Effect of Leading-Edge Separation on the Lift of a Delta Wing," *Journal of Aeronautical Sciences*, Vol. 21, No. 90, Oct. 1954, pp. 690-694.
- Squire, L. C., Jones, J. G., and Stanbrook, A., "An Experimental Investigation of the Characteristics of Some Plane and Cambered  $65^\circ$  Delta Wings at Mach Numbers From 0.7 to 2.0," ARCR&M 3305, 1963.
- Love, E. S., "Investigations at Supersonic Speeds of 22 Triangular Wings Representing Two Airfoil Sections for Each at 11 Apex Angles," NACA Rept. 1238, 1955.
- Miller, D. S. and Wood, R. M., "An Investigation of Wing Leading-Edge Vortices at Supersonic Speeds," AIAA Paper 83-1816, July 1983.
- Stanbrook, A. and Squire, C. C., "Possible Types of Flow at Swept Leading Edges," *Aeronautics Quarterly*, Vol. XV, Feb. 1964, pp. 72-82.
- Wood, R. M. and Miller, D. S., "Assessment of Preliminary Prediction Techniques for Wing Leading-Edge Vortex Flows at Supersonic Speeds," AIAA Paper 84-2208, Aug. 1984.
- Hitzel, S. M. and Schmidt, W., "Slender Wings with Leading-Edge Vortex Separation—A Challenge for Panel-Methods and Euler Codes," AIAA Paper 83-0562, Jan. 1983.
- Newsome, R. W., "A Comparison of Euler and Navier-Stokes Solutions for Supersonic Flow Over a Conical Delta Wing," AIAA Paper 85-0111, Jan. 1985.
- Wardlaw, A. B. Jr., Hackermann, L. B., and Baltakis, F. P., "An Inviscid Computational Method for Supersonic Missile Type Bodies—Program Description and User's Guide," NSWC TR-81-459, Dec. 1981.
- Rizzi, A., "Euler Solutions of Transonic Flow Around the Dillner Wing—Compared and Analyzed," AIAA Paper 84-2142, Aug. 1984.
- Murman, E. M., "Solutions of the Conical Euler Equations for Flat Plate Geometries—Preliminary Results," Massachusetts Institute of Technology, Cambridge, Mass., CFDL-TR-84-4, Aug. 1984.
- Polhamus, E. C., "Predictions of Vortex-Lift Characteristics by a Leading-Edge Suction Analogy," *Journal of Aircraft*, Vol. 8, April 1971, pp. 193-199.
- Carlson, H. W. and Mack, R. J., "Estimation of Wing Nonlinear Aerodynamic Characteristics at Supersonic Speeds," NASA TP-1718, Nov. 1980.
- Lan, E. E. and Chang, J. F., "Calculation of Vortex Lift Effect for Cambered Wings by the Suction Analogy," NASA CR-3449, 1981.